Journal of Physiology (1991), **440**, *pp.* 95–112
With 8 figures
Printed in Great Britain

THE ROLE OF THE β_4-SUBUNIT IN DETERMINING THE KINETIC PROPERTIES OF RAT NEURONAL NICOTINIC ACETYLCHOLINE α_3-RECEPTORS

BY ROGER L. PAPKE* AND STEPHEN F. HEINEMANN

From the Molecular Neurobiology Laboratory, The Salk Institute, PO Box 85800, San Diego, CA 92186, USA

(*Received 5 November 1990*)

SUMMARY

1. Single-channel currents were recorded from *Xenopus* oocytes which had been injected with complementary RNAs (cRNAs) for the neuronal nicotinic acetylcholine receptor subunits α_3 and β_4. The co-expression of α_3 and β_4 gave rise to three different channel types with conductances of 22, 18 and 13 pS.

2. The activity arising from the expression of these two subunits was compared with that observed when the α_3 subunit was co-expressed with an alternative β-subunit, β_2. The $\alpha_3\beta_4$-receptors differed from $\alpha_3\beta_2$-receptors in conductance, open times and most notably, in burst kinetics. The association of the β_4-subunit with the α_3-subunit results in receptors which have a high probability of re-opening after closing, yielding protracted bursts of activity not observed when the α_3-subunit is associated with the β_2-subunit.

3. All three $\alpha_3\beta_4$-channel types had similar burst kinetics. However, the 13 pS conductance channels showed an additional long-lived open state to varying degrees when clusters of activity within an individual record were examined.

INTRODUCTION

Functional diversity of synaptic receptors for a particular neurotransmitter can arise as a consequence of the differential or developmentally regulated expression of related genes. Such a family of related genes exists for neuronal nicotinic acetylcholine receptors (AChR) (Boulter, Connolly, Deneris, Goldman, Heinemann & Patrick, 1987; Duvoisin, Deneris, Patrick & Heinemann, 1989), and in general, functional receptors are believed to arise from the co-expression of α- and β-subunits (Connolly, 1989; see also Couturier, Bertrand, Matter, Hernandez, Bertrand, Millar, Valera, Barka & Ballivet, 1990*a*). The class of neuronal nicotinic subunits which are identified as α-subunits are believed to be the agonist-binding subunits of neuronal nicotinic receptors based on their structural homology to the muscle AChR α-subunit (α_1) in the region of the agonist binding site (Boulter, Evans, Goldman, Martin, Treco, Heinemann & Patrick, 1986). Three neuronal α-subunits (α_2, α_3, and α_4) have

* To whom correspondence should be addressed.

MS 8915

been isolated which form functional nicotinic receptors when co-expressed in *Xenopus* oocytes with either of two neuronal β-subunits (β_2 or β_4) (Boulter *et al.* 1987; Deneris, Connolly, Boulter, Patrick & Heinemann, 1988; Wada, Ballivet, Boulter, Connolly, Wada, Deneris, Boulter, Swanson, Heinemann & Patrick, 1988; Duvoisin *et al.* 1989). The nicotinic acetylcholine receptor subunits β_2 and β_4 are believed to be functional homologues of the muscle β-subunit β_1, since either can substitute for the β_1 subunit when co-expressed with α_1-, γ- and δ-subunits of the muscle AChR to allow for the formation of functional chimaeric muscle–neuronal nicotinic receptors (Deneris *et al.* 1988; Duvoisin *et al.* 1989).

The β-subunits influence numerous properties of the nicotinic response in oocytes. For example, oocytes injected with complementary RNAs (cRNAs) for the $\alpha_3\beta_2$ and $\alpha_3\beta_4$ nicotinic subunits have different macroscopic dose–response relationships with the $\alpha_3\beta_4$-receptors showing a higher apparent dissociation constant (K_d) and a steeper dose–response relationship than $\alpha_3\beta_2$-receptors (R. L. Papke, unpublished observation; Luetje & Patrick, 1991; similar finding reported for chick receptors by Couturier, Erkamn, Valera, Rungger, Bertrand, Boulter, Ballivet & Bertrand, 1990*b*). $\alpha_3\beta_2$-and $\alpha_3\beta_4$-receptors also respond differently to neuronal bungarotoxin (bungarotoxin 3.1). Neuronal bungarotoxin, which is believed to be a competitive antagonist, effectively blocks $\alpha_3\beta_2$-receptors but is unable to block the responses of $\alpha_3\beta_4$-receptors (Duvoisin *et al.* 1989).

In situ hybridization experiments have indicated that each of the neuronal nicotinic subunit genes has a unique pattern of expression in the nervous system (Goldman, Deneris, Kochhar, Boulter, Patrick & Heinemann, 1987; Duvoisin *et al.* 1989; Wada, Wada, Boulter, Deneris, Heinemann, Patrick & Swanson, 1989). Of the α-subunits, the α_4-subunit has the highest level of expression in the brain, being expressed in many regions. The α_2- and α_3-subunit genes are found in more restricted portions of the brain. The β_2-subunit is also widely expressed throughout the brain, apparently co-expressed with the α-subunits. Transcription of the β_4-subunit gene in the brain however is largely restricted to the ventral portion of the medial habenula (Duvoisin *et al.* 1989). These observations suggested that in general the functional diversity of nicotinic receptors in the brain might arise from the co-expression of different α-subunits along with the β_2-subunit. Indeed, we have shown that the three α-subunits give rise to functionally distinct receptors when each is co-expressed with the β_2-subunit (Papke, Boulter, Patrick & Heinemann, 1989). Our experiments also indicated that a heterogeneous population of receptors arises from the pairwise expression of the β_2-subunit and any single α-subunit in oocytes, suggesting that, in this system, receptors are formed that vary in the arrangement or stoichiometry of the subunits or in their post-translational modifications. In the case of $\alpha_2\beta_2$-receptors, the presence of the channel type with low conductance was enhanced when excess message for the β_2-subunit was injected (Papke *et al.* 1989).

In the brain the α_4-subunit is the most widely expressed α-subunit and the β_2-subunit is the predominant β-subunit. In the peripheral nervous system other subunits appear to play important roles. Specifically, the β_4-subunit is widely expressed in peripheral nervous tissues, and the predominant α-subunit gene expressed in autonomic ganglia is the α_3-subunit (I. Hermans-Borgmeyer, personal communication). In order to investigate the functional significance of this pattern of

subunit gene expression, single-channel currents were recorded from *Xenopus* oocytes which had been injected with *in vitro*-transcribed RNAs (cRNA) coding for the α_3- and β_4-subunits. In this paper we report the kinetic properties of the receptors formed by the expression of these subunits. By comparing the currents observed with those arising from the co-expression of the α_3- and β_2-subunits, we identify potential functional roles for the different β-subunits of the neuronal nicotinic receptor family.

METHODS

In vitro RNA transcripts were made from the cDNA clones for the α_3- and β_4-subunits and stored at −70 °C until use. *Xenopus laevis* oocytes were obtained and prepared as previously published (Papke *et al.* 1989) from frogs anaesthetized with MS-222. On the day following surgical removal, the oocytes were injected with 3–6 ng of cRNA for each subunit per oocyte. Two days after injection, oocytes were screened by voltage recordings for the expression of functional receptors. Batches of oocytes which showed robust depolarizing responses to the application of acetylcholine were used for patch clamp recordings. Experiments were conducted at room temperature (23–25 °C), and frog Ringer solution (115 mM-NaCl, 10 mM-HEPES, 2·5 mM-KCl and 1·8 mM-$CaCl_2$) with 0·5 μM-atropine was used both in the electrode and in the bath. Standard patch clamp procedures (Hamill, Marty, Neher, Sakmann & Sigworth, 1981) were applied as previously described (Papke *et al.* 1989) and all data reported were acquired in the cell-attached configuration with either 1 or 10 μM-ACh in the pipette. Control recordings were made from uninjected or sham-injected oocytes as described by Papke *et al.* (1989).

Electrodes were fabricated from Dagan thick-wall, hard glass SG-16 capillaries and were Sylgard coated and fire-polished before use. Data were acquired with a Dagan 8900 patch clamp amplifier (50 GΩ head stage), filtered initially at 10 kHz (−3 dB value, 8-pole Bessel filter), digitized, and stored on VCR tape. For analysis, data were refiltered at 4 kHz, sampled at 20 kHz and selectively stored in the memory of a PC AT computer using an event detector (Axon Instruments) and a LabMaster (Tecmar) analog-to-digital conversion system (for details see Papke *et al.* 1989). Digitized records were analysed using the pClamp software package (Axon Instruments), version 5.03 or later. The pClamp program fits event duration distributions with a non-linear least-squares method using a Levenberg–Marquardt fitting algorithm.

Open time duration distributions (events $\geqslant$ 100 μs) were fitted to either two or three exponential components using the standard binning procedures available in pClamp. It should be noted that these represent *apparent open times* since gaps less than 100 μs were ignored. Amplitude distributions were constructed including only those events of sufficient duration to have reached full amplitude, given the 4 kHz filtering ($>$ 400 μs). Channel conductances were calculated by linear regression analysis of the values obtained from the fit of amplitude distributions for the same patch at three or more voltages within the range of 0–100 mV hyperpolarized from resting potential. When multiple conductances were present in a patch, the amplitude threshold for the creation of idealized records was set for the smallest observed conductance to maximize the sampling of all channel amplitudes. When multiple peaks were observed in the event amplitude distributions it was sometimes difficult to deduce the correct current–voltage relationships of those channels present in the patch, and the data were rejected. Also, when multiple channel types were present, event duration distributions were not analysed. In this paper we report data from a total of sixteen patches from $\alpha_3\beta_4$ subunit-injected oocytes. In fourteen patches a single conductance was identified, and in the remaining two patches a small-conductance (13 pS) channel was present initially along with a channel of larger conductance. In the event amplitude distributions at all voltages the low-conductance channel was associated with peaks that represented small fractions of the total area of the distributions. A non-stationary (i.e. decreasing) frequency of events is characteristic of these channels (see Papke *et al.* 1989), and the 13 pS conductance channel appeared to inactivate (or desensitize) more rapidly than the large channel and was absent from the latter portions of the recording.

Burst analysis was conducted on Macintosh computers after the idealized records generated by pClamp were converted to the appropriate format using Apple file conversion software. The idealized records were imported into Excel (Microsoft), and lists of burst durations were

constructed with a macro (written by Don Fredkin, UCSD Physics Department, San Diego, CA, USA) that defined bursts as periods of activity when openings were separated by closed time less than or equal to some burst threshold. In order to examine the dependence of burst features on the size of the threshold value, bursts were defined with thresholds of 1, 4, 12 and 100 ms. Lists of open times and burst durations were then subjected to a log transform (Sigworth & Sine, 1987) and the peaks of the log duration distributions were identified. Burst duration distributions had two components, and we report the mean value of the long burst durations (from the log transforms) and the relative number of events that were associated with that component. For comparison, idealized records of recordings obtained from $\alpha_3\beta_2$-subunit-injected oocytes (Papke *et al.* 1989) were also analysed in the same manner.

Closed time distributions were fitted using the log transformations of the idealized records available in pClamp (version 5.5.1). The fitting statistics of the open time distributions were also generated by the pClamp pStat module. Analysis of event duration or burst duration distributions were done for each patch on records obtained at different voltages, and then average values were generated for each patch. The patches were then classified based on channel conductance and/or agonist concentration (as noted in the text), and the values reported are the averages ($\pm$S.E.M.) of multiple patches of the same classification.

A simple scheme for burst behaviour was used to model the data (see Discussion) and rate constants were calculated for each patch based on the closed time and burst duration distributions with a 4 ms threshold. Based on the analysis of $\alpha_3\beta_4$-subunit closed time distributions (calculated as in Jaramillo & Schuetze, 1988), with this threshold approximately only 3·1 % of the $\tau_{c,1}$- and $\tau_{c,2}$-type closures will be misassigned as interburst closures and 4·1 % of the $\tau_{c,3}$- and $\tau_{c,4}$-type closures will be misassigned as intraburst closures. $\tau_{c,1}$–$\tau_{c,4}$ are time constants for closed time distributions. Only data obtained in the presence of 1 μM-ACh were used for these calculations. The values reported represent the averages of multiple patches. In order to calculate rate constants, we made a simplifying assumption based on the observation that channel activation, in general, occurred either as isolated brief events or as long bursts. We took all brief bursts to be bursts of a single event. We then were able to calculate the number of openings per long burst from the ratio of openings to bursts and the percentage of bursts which were of long duration. For example, if there were 400 openings, 150 bursts, and 50 % of all bursts were long, then we estimated seventy-five long bursts with an average of 4·33 (325/75) openings per long burst (3·33 gaps per long burst). Given the relative areas of the τ_1 and τ_2 components of the closed time distributions, the number of interruptions ($\tau_{c,1}$, see text) and the number of true closures ($\tau_{c,2}$) were then calculated. The rate of transitions into the $\tau_{c,1}$ closed state (the forward interruption rate, I_f) was calculated as the number of $\tau_{c,1}$ closures per burst divided by the burst duration, and the closing rate (α) was calculated from the number of $\tau_{c,2}$ closures per burst divided by the burst duration. The duration of $\tau_{c,2}$ was taken to equal $1/(\beta + k^-)$ (where β is the rate of channel opening and k^- is the dissociation rate) and the number of $\tau_{c,2}$ closures per burst as β/k^-. The backward interruption rate (I_b) was calculated as $1/\tau_{c,1}$.

RESULTS

General features

The acetylcholine-induced single-channel activity in cell-attached patches on oocytes injected with cRNA coding for the α_3- and β_4-subunits shared some general features with what has been previously reported for currents that arise from the co-expression of α-subunits with the β_2-subunit (Papke *et al.* 1989). In general the event frequency decreased with time and in many cases the frequency of events fell to zero after several minutes of recording. As was observed with receptors formed with the β_2-subunit, $\alpha_3\beta_4$-receptors were not active when the patch was held at depolarized potentials. Measurements of conductance, mean channel open time and other kinetic parameters demonstrated that the co-expression of the α_3- and β_4-subunits gave rise to more than a single type of channel. Similar observations have been reported for receptors formed from the expression of the α_3-subunit (or the other α-subunits) along with the β_2-subunit. Although in some cases multiple channel types were

observed in the same patch, patches usually had activity arising from a single channel type. If a patch had multiple channel types, direct transitions between conductance levels were not observed and, likewise, activity within bursts was always of the same type. These features led us to suggest (Papke *et al.* 1989) that the

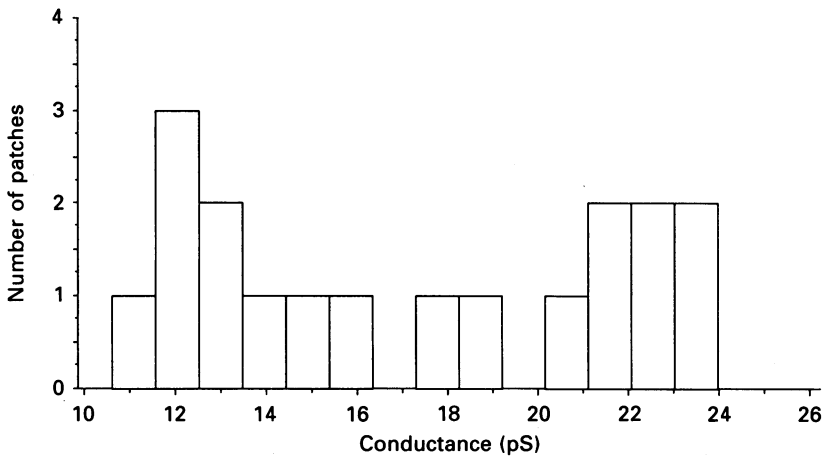

Fig. 1. Histogram of the single-channel conductances identified in sixteen cell-attached patches from oocytes injected with *in vitro*-transcribed RNA for the neuronal nicotinic α_3- and β_4-subunits. Bins on the x-axis are the single-channel conductances which were calculated as described in Methods. The y-axis gives the number of channels per bin. Based on conductances (γ), three channel types were identified: primary type, $\gamma = 22{\cdot}4 \pm 0{\cdot}4$ pS ($n = 7$); secondary type, $\gamma = 13{\cdot}0 \pm 0{\cdot}5$ pS ($n = 9$); tertiary type, $\gamma = 17{\cdot}9 \pm 0{\cdot}5$ pS ($n = 2$).

different channel types arising from the expression of the same genes were associated with channels that had different structures, i.e. different subunit stoichiometry or post-translational modifications.

Conductances and open times

In Fig. 1 we display the distribution of conductances observed in oocytes injected with cRNA for the α_3- and β_4-subunits. Two channel conductance types were most frequently observed; a large channel type ($n = 7$) which had an average conductance of $22{\cdot}4 \pm 0{\cdot}4$ pS, and a small channel type ($n = 9$) with an average conductance of $13{\cdot}0 \pm 0{\cdot}5$ pS. Based on the terminology we established previously for the multiple channel types observed when the β_2-subunit was expressed with the different α-subunits, we will refer to the large (22·4 pS) conductance channel as the primary channel type and the small (13·0 pS) channel as the secondary channel type. Additionally, a third channel type was infrequently observed ($n = 2$) which had an intermediate conductance of $17{\cdot}9 \pm 0{\cdot}5$ pS. Although this distinction of a tertiary channel type is based on just two observations, the channels of this type had properties which were distinct from the other channel types (see Fig. 5).

The open time distributions were fitted to two exponentials, and the average values for the three channel types are given in Table 1, along with the conductance

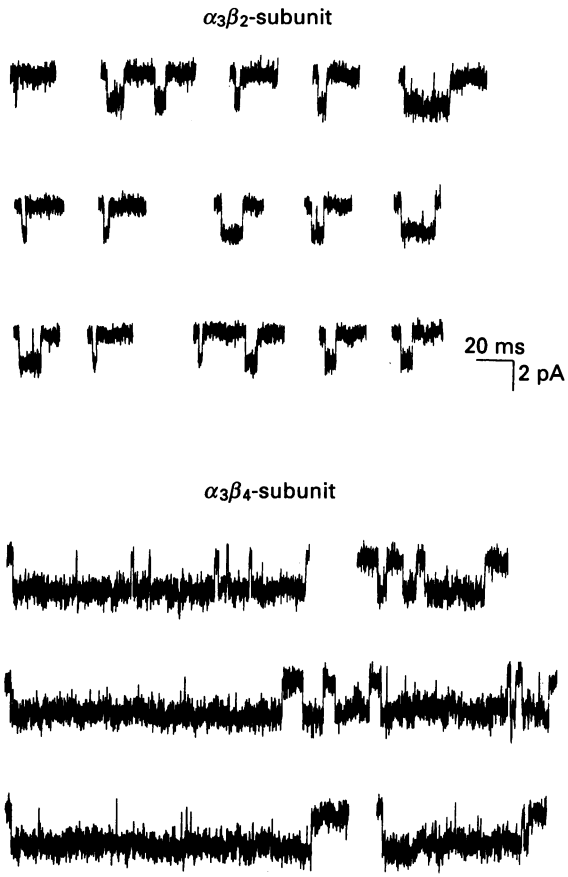

Fig. 2. Single-channel events chosen to illustrate the difference between the nature of the long bursts of $\alpha_3\beta_2$-channels and $\alpha_3\beta_4$-channels. The data were obtained in the presence of 1 μM-ACh and at holding potentials between 40 and 60 mV hyperpolarized from rest.

TABLE 1. Single-channel properties of nicotinic acetylcholine receptors

Receptor subunits	Channel type	Conductance (pS)	n for I–V	Brief open times (ms)	Long open times (ms)
$\alpha_3\beta_2$	Primary	15·4 ± 0·8	10	0·22 ± 0·03	4·0 ± 0·2
	Secondary	5·1 ± 0·4	3	0·09 ± 0·01	1·6 ± 0·3
$\alpha_3\beta_4$	Primary	22·4 ± 0·4	9	0·38 ± 0·07	7·2 ± 2·1
	Secondary	13·0 ± 0·5	7	0·33 ± 0·05	5·5 ± 1·4
	Tertiary	17·9 ± 0·5	2	0·36 ± 0·02	5·8 ± 0·7

Comparison of the single-channel properties of nicotinic acetylcholine receptors formed by the expression of the rat α_3-subunit in *Xenopus* oocytes, in combination with either the β_2- or β_4-subunit. Data on $\alpha_3\beta_2$-subunit combination from Papke *et al.* (1989). n = number. Values are means ± S.E.M.

and open times reported for the channels formed by the expression of α_3- and β_2-subunits. In general, the expression of the β_4-subunit gave rise to channels of larger conductance and longer open time than those formed with the β_2-subunit.

Bursts analysis

Although the primary channel type formed from α_3- and β_4-subunits can be distinguished from $\alpha_3\beta_2$-receptors based on differences in conductance and open time, the secondary $\alpha_3\beta_4$-channel type has a conductance and open time similar to the

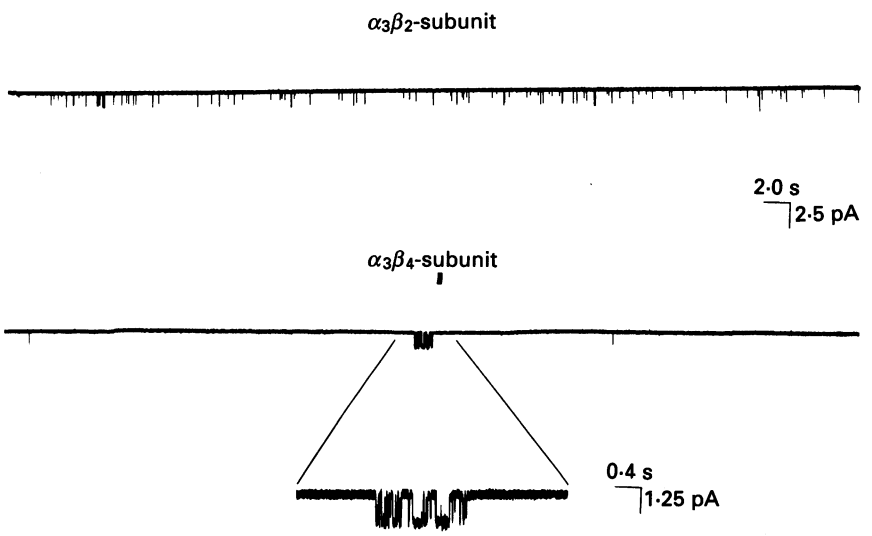

Fig. 3. Recordings of single-channel activity from oocytes injected with RNA coding for either the α_3- and β_2-subunits (upper trace) or the α_3- and β_4-subunits (lower trace). Both recordings were made in the presence of 1 μM-ACh with a holding potential of 50 mV hyperpolarized from rest, and display a total of $\approx$ 200 events. For this figure the data were replayed from the video cassette recording (filtered at 1 kHz) and plotted with a chart recorder. The temporal resolution of this figure, however, was effectively limited to that of the response frequency of the chart recorder, $\approx$ 500 Hz; consequently, relatively brief events appear to be less than their full amplitude.

primary $\alpha_3\beta_2$-channel type. Even so, the $\alpha_3\beta_4$-receptor currents for all three channel types are clearly different when they are analysed in terms of their activation mechanisms. Specifically, the events arising from $\alpha_3\beta_4$-channels often occur as protracted bursts of activity, while $\alpha_3\beta_2$-receptors have a much lower tendency to re-open after closing. This is illustrated in Fig. 2. Furthermore, the activation of $\alpha_3\beta_2$-receptors is evenly spaced throughout a recording (except for the run-down tendency noted above), while the activation of $\alpha_3\beta_4$-receptors is periodic, with long periods of time when there are only rare isolated openings followed by intervals when the channels are intensely active (clusters of bursts). This difference in receptor activation associated with the expression of β-subunits is illustrated in Fig. 3, which compares the distribution of activity arising from an $\alpha_3\beta_2$- (primary type) receptor with that of an $\alpha_3\beta_4$- (primary type) receptor over the course of 1 min. Both recordings were made in the presence of 1 μM-ACh, with a holding potential of 50 mV, hyperpolarized from rest, and display roughly the same number of events.

We conducted a burst analysis of recordings obtained from oocytes injected with either α_3- and β_2- or α_3- and β_4-subunits. Bursts were defined as periods of activity

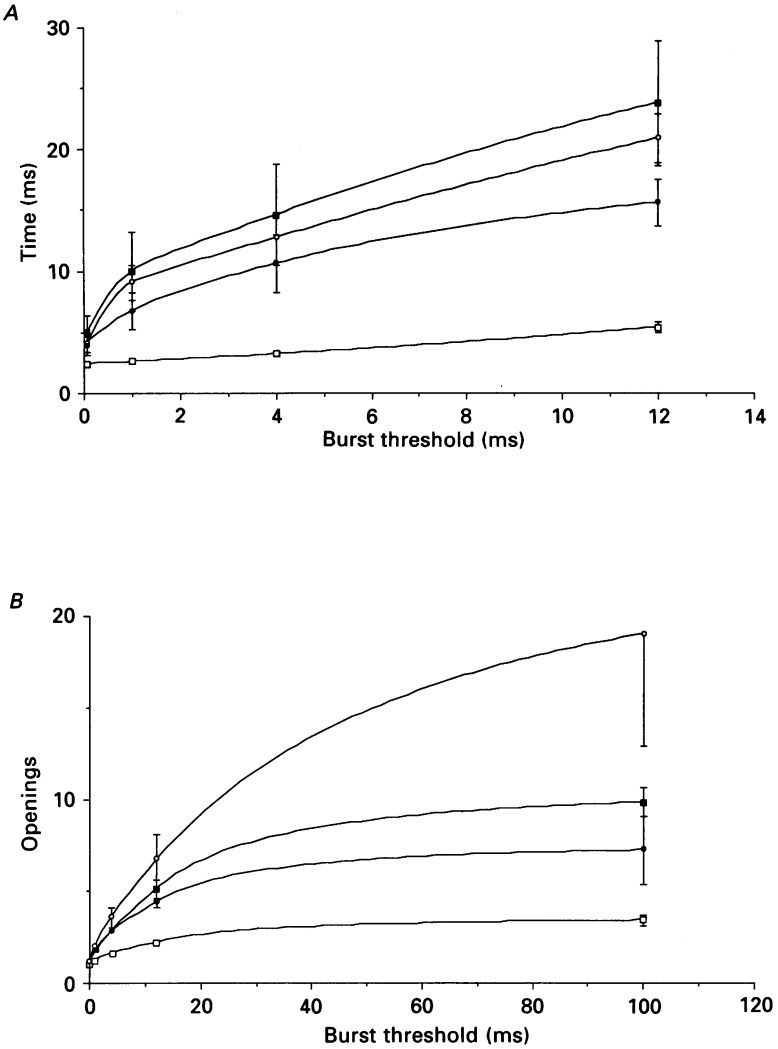

Fig. 4. Burst analysis of single-channel activity arising from the expression of either the $\alpha_3\beta_2$-subunits or $\alpha_3\beta_4$-subunits. The average values for each of the three types of $\alpha_3\beta_4$-channels are plotted as well as the average values of $\alpha_3\beta_2$-subunit primary type channels ($n = 7$). ■ represent $\alpha_3\beta_4$-channels of the primary type, ○ represent $\alpha_3\beta_4$-channels of the secondary type, ● represent $\alpha_3\beta_4$-channels of the tertiary type, and □ represent $\alpha_3\beta_2$-channels of the primary type. The line plotted through the points is an interpolation provided to facilitate the identification of the values for each channel type. *A*, long burst durations as a function of burst threshold (see Methods) with burst thresholds of 1, 4 or 12 ms. *B*, the ratio of openings to bursts (total) with burst thresholds of 1, 4, 12, or 100 ms. Error bars show S.E.M.

separated by closed times less than some threshold (t_c). Thresholds tested were 1, 4, 12 and 100 ms (see Methods). This analysis gave values for burst durations and the number of openings per burst for each of the channel types. The burst duration distributions had two components, one associated with isolated, brief events and the other associated with long bursts. Plotted in Fig. 4*A* is the average duration of long

bursts (with thresholds of 1, 4 or 12 ms) arising from each of the channel types, while Fig. 4*B* plots the ratio of openings to bursts (with thresholds of 1, 4, 12, or 100 ms). Regardless of the threshold value, burst analysis defines periods of activation much longer for all three types of $\alpha_3\beta_4$-channels than for $\alpha_3\beta_2$-channels (at most points

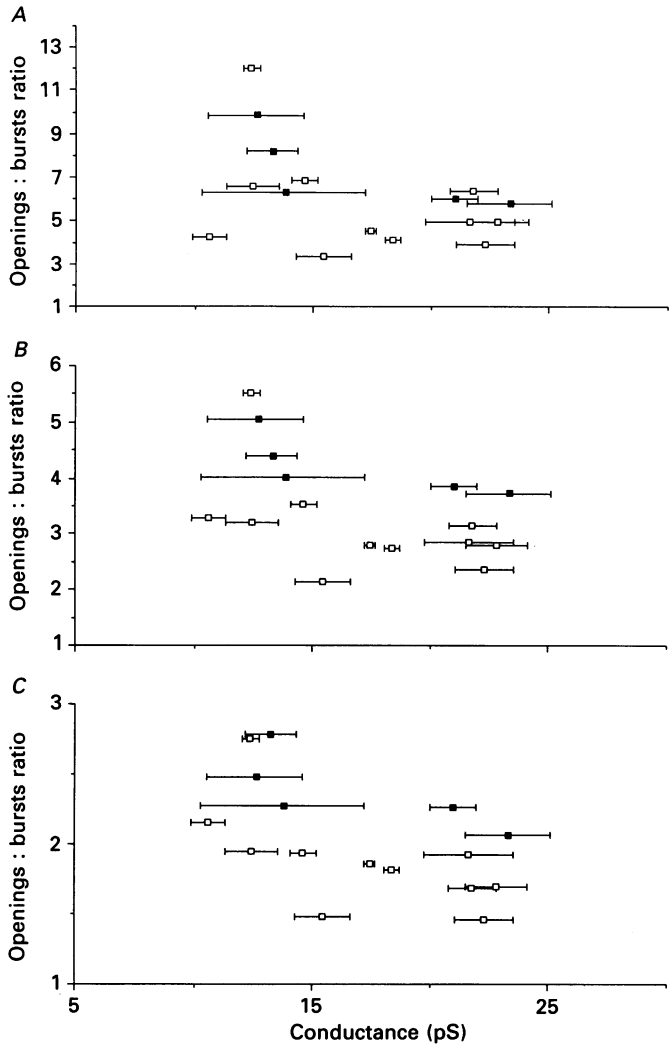

Fig. 5. Scatter plots of the ratio of openings to bursts (y-axis) *vs.* conductance (x-axis) for $\alpha_3\beta_4$-receptors. The three plots represent data from the same patches with different values for the burst thresholds. In *A*, *B* and *C* the burst thresholds were 12, 4 and 1 ms respectively. The error bars represent the standard errors of the mean on the slope of the *I–V* data for each individual patch. Data obtained in the presence of 1 μM-ACh (□), and 10 μM-ACh (■).

$P < 0{\cdot}001$). With thresholds up to 12 ms, the average burst durations defined by this analysis yield values between 10 and 20 ms. In the presence of 1 μM-ACh, with thresholds of up to 100 ms, all types of $\alpha_3\beta_4$-channels also show far more openings per

burst than $\alpha_3\beta_2$-channels ($P < 0.01$ at all points). At the longest threshold tested (100 ms), the secondary channel types appear to have more openings per burst than the other $\alpha_3\beta_4$-channel types. However, this difference is not significant due to variability in the burst behaviour of the secondary channel type (see below).

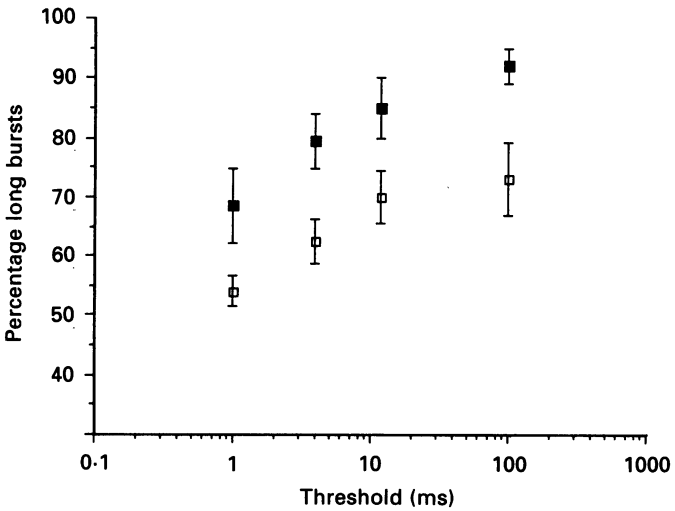

Fig. 6. Plots of the percentage of events in the burst duration distributions which were identified as long bursts at increasing values of burst threshold (log scale). Data are plotted for $\alpha_3\beta_4$-channels at either 1 μM-ACh (□) or 10 μM-ACh (■). Means ± S.E.M.

Effect of agonist concentration

Some recordings from $\alpha_3\beta_4$-injected oocytes were obtained in the presence of 10 μM-ACh, and while the average duration of long bursts was not affected by agonist concentration (data not shown) the ratio of openings to bursts tended to be greater at higher agonist concentration (see Fig. 5). This observation was related to the fact that at high agonist concentrations there were fewer isolated brief events and a larger percentage of long bursts (see Fig. 6). Similar influences of agonist concentration on the ratio of brief and long bursts has been observed with many preparations of muscle AChR (Takeda & Trautmann, 1984; Colquhoun & Sakmann, 1985; Labarca, Montal, Lindstrom & Montal, 1985; Papke & Oswald, 1989). Note that with $\alpha_3\beta_4$ channels (data from all types have been pooled in Fig. 6) the burst analysis define a relatively constant percentage of long bursts, even with thresholds up to 100 ms.

Burst mechanisms: closed time distributions

In order to further study the burst kinetics of the $\alpha_3\beta_4$-channels, closed time distributions were analysed. Distributions were well fitted by four exponential components. When the average values were calculated separately for each of the three different $\alpha_3\beta_4$-channel types at the same agonist concentration (data not shown) comparable distributions were produced, suggesting that the bursts of all $\alpha_3\beta_4$-channels arise from similar mechanisms. Figure 7 displays the closed time data

averaged from all $\alpha_3\beta_4$-channel types compared to the closed time data from seven patches with primary type $\alpha_3\beta_2$-channels. The major difference in the closed time distributions, associated with the expression of different β-subunits, is that the $\alpha_3\beta_4$-receptors show a large percentage of the closed times fitted to the two components of

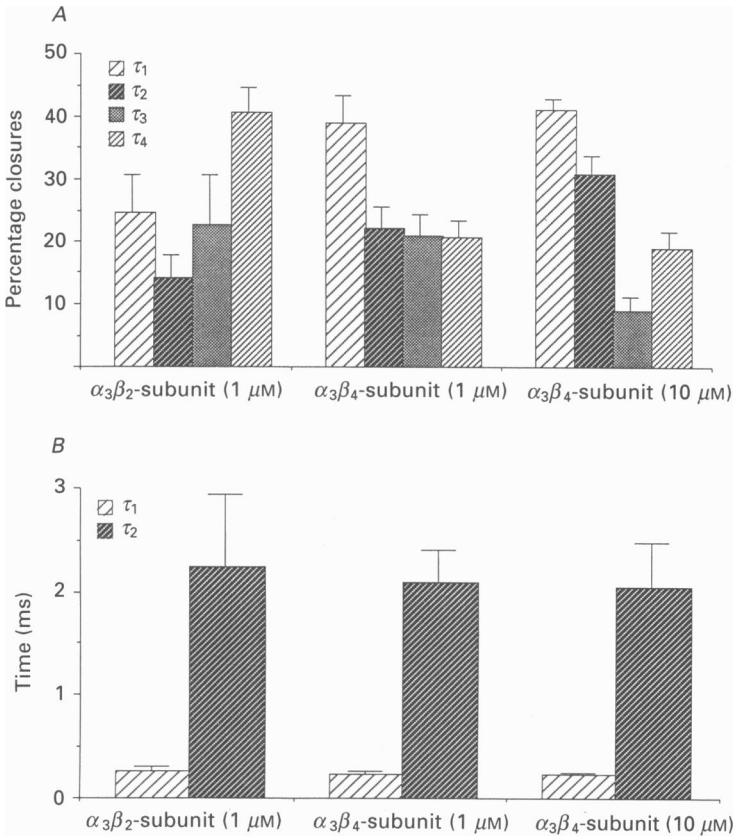

Fig. 7. Closed time distributions of $\alpha_3\beta_2$-channels or $\alpha_3\beta_4$-channels at either 1 μM-ACh or 10 μM-ACh. *A*, the relative areas of the closed time distributions fitted to the four exponential components of the closed time distributions (τ_1, τ_2, τ_3, and τ_4). *B*, the time constants of the two most brief components of the closed time distributions (τ_1 and τ_2). Means $\pm$ S.E.M.

brief duration, presumably representing two types of intra-burst closures ($\tau_{c,1}$ = 0·194 $\pm$ 0·029 ms and $\tau_{c,2}$ = 2·05 $\pm$ 0·31 ms). Although there were more closures fitted to the $\tau_{c,1}$ and $\tau_{c,2}$ components in the closed time distributions of $\alpha_3\beta_4$-channels, the time constants of these components were not different from the $\alpha_3\beta_2$-subunit distributions ($\tau_{c,1}$ = 0·220 $\pm$ 0·050 ms and $\tau_{c,2}$ = 2·20 $\pm$ 0·70 ms). When the closed time distributions obtained from $\alpha_3\beta_4$-channels in the presence of 10 μM-ACh were examined, the relative area of the two fast components was further increased due to the increased percentage of long bursts as noted above. The time constants for the $\tau_{c,1}$ and $\tau_{c,2}$ components of the $\alpha_3\beta_4$-subunit distributions were also unaffected by agonist concentration. The time constants for the $\tau_{c,3}$ and $\tau_{c,4}$ components may have

been influenced by subunit composition and agonist concentration (data not shown); however the variability in these values between patches and through the course of a recording (due to the non-stationary frequency of events) makes the interpretation of these values difficult.

Three exponential fits of open time

Although the burst duration distributions seemed well described by two components, some of the $\alpha_3\beta_4$-subunit log open time distributions appeared to have three components, suggesting that one or more of the channel types might exhibit three open states. To test this, open time distributions obtained in the presence of 1 μM-ACh were fitted to either two or three exponential components, and the improvement in fit was evaluated by calculating a fit improvement ratio (FIR) for each distribution.

$$\text{FIR} = \frac{\chi^2 \text{ for two-exponential fit/degrees of freedom}}{\chi^2 \text{ for three-exponential fit/degrees of freedom}}.$$

While there was only a small improvement in fit for patches with the primary channel type (average FIR = $1{\cdot}64 \pm 0{\cdot}37$, $n = 4$), overall there was a much greater improvement in fit for patches with the secondary channel type (average FIR = $12{\cdot}7 \pm 4{\cdot}3$, $n = 5$). However, the improvement in fit was not a consistent feature of all patches with the secondary type channels, nor was it consistent for a given patch between recordings made at different potentials. Four out of five recordings of the secondary channel type showed a significant overall improvement (average FIR = $15{\cdot}7 \pm 4{\cdot}0$, $n = 4$), and the other patch had no improvement (average FIR = $0{\cdot}845 \pm 0{\cdot}07$). Of the four patches which showed an overall improvement in fit, the values of the FIR for individual distributions varied from 0·896 to 48·1. This suggested that the behaviour of these secondary type channels might not be stationary, or that the activity in a patch might arise from multiple channels in a patch that differed in open time. Although the majority of these recordings had no multiple events, in some recordings a small number of overlapping events was observed ($\leqslant 3{\cdot}2\%$), providing evidence that at least in some cases more than one channel was present in the patch.

As noted above, the activity in these records was grouped in well-defined clusters (see Fig. 8). If multiple channels were present in a patch, then an improvement in the fit with three exponentials might reflect activity arising from two channels with similar brief open times and different long open times. If this were the case, then individual clusters might be fitted by two exponentials and the overall distribution much better fitted by three. Figure 8*A* is a scatter plot of open time *vs.* cumulative time in a recording from a patch where no multiple events were observed. A total of 787 events are plotted of which $> 96\%$ occur within the five clusters outlined. These clusters represent $< 31\%$ of the total time within the recording. Overall, the open time distribution had a FIR = 21·3.

We examined the FIR of each cluster to test whether individual clusters were well fitted by two components or were significantly improved by fitting three components. While there was no improvement in the fit of the first cluster (FIR = 1·0) there was

increasing improvement in the fit of clusters 2–5 (Fig. 8*B*). This increase in the FIR of individual clusters could be described by an exponential function ($R^2 = 0{\cdot}993$) with a time constant of $\approx$ 15 s. This increase in the FIR may have been associated with the increased presence of a new long open time. Also plotted in Fig. 8*B* is the

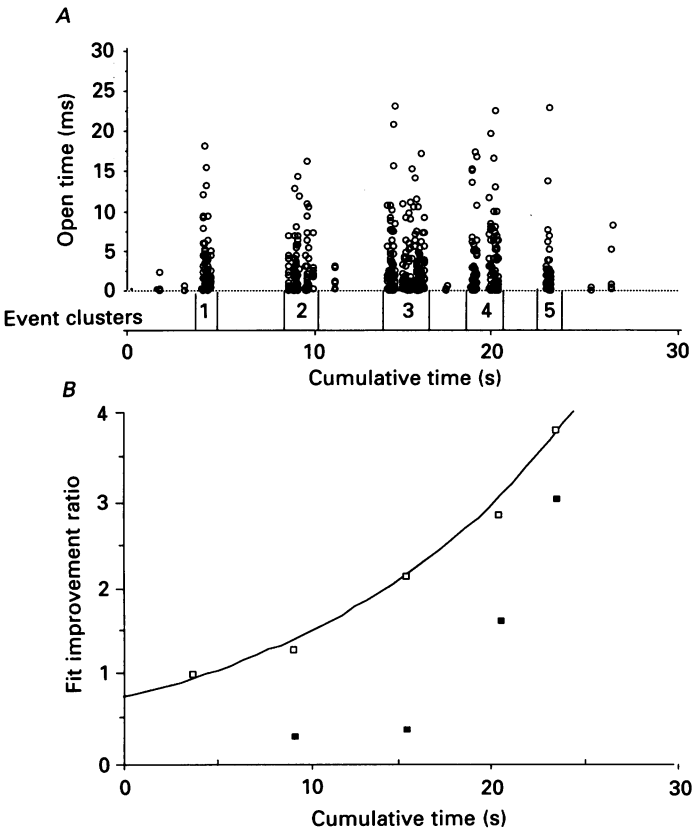

Fig. 8. Analysis of activity within clusters of bursts in a continuous record. *A*, a scatter plot of open time *vs.* cumulative time (in ms) for all of the events in an idealized record of the activity arising from an $\alpha_3\beta_4$-subunit secondary type channel in the presence of 1 μM-ACh at a holding potential 40 mV hyperpolarized from rest. Five clusters of activity (1–5) are defined by the lines below the plot. *B*, the 'fit improvement ratio' (FIR, see text) of the five clusters illustrated in the upper plot are represented by □ plotted as a function of cumulative time (in s). The line represents an exponential fit of the increase in FIR over time ($\tau \approx 15$ s). ■ represent the ratio of the area of the longest component (τ_3) of the three-exponential fit of the open time distribution to the area of the intermediate component (τ_2) for those clusters where the FIR > 1.

ratio of the areas of the third (longest) component and the second (intermediate) component of the three exponential fits for those clusters when the FIR was greater than 1. Along with the increased appearance of a third open state, the duration of long bursts also increased between the five clusters. For clusters 1–5 the average long burst duration from the log transforms of the burst duration distributions were 24·3, 37·1, 40·6, 41·3, and 50 ms respectively (threshold = 12 ms).

DISCUSSION

In this paper we have shown that β_2- and β_4-subunits have important effects on the activation kinetics of neuronal nicotinic receptors. The differential expression of these nicotinic acetylcholine receptor subunit genes may influence developmental and tissue-specific aspects of cholinergic function. While the properties of these receptors formed in oocytes cannot be directly related to particular nicotinic receptors found *in vivo*, we chose to study the effects that these two different non-α-subunits have on the properties of receptors formed with the α_3-subunit, because these combinations may be relevant to differences in nicotinic function between the CNS and the autonomic nervous system. The β_2-subunit is co-expressed with the α_3-subunit at sites in the brain, but the α_3-subunit is the predominant α-subunit in the peripheral nervous system, where it is usually co-expressed with the β_4-subunit.

Our data suggest that while the α_3-subunit forms receptors with the β_2-subunit which have rapid kinetics of inactivation, when expressed with the β_4-subunit, the α_3-subunit forms receptors which have distinctive bursting kinetics, resulting in prolonged periods of activation. This implies that the expression of the β_2-subunit may be important at sites where rapid synaptic integration is required, and that the expression of the β_4-subunit may be fundamental to the production of prolonged or sustained responses in tissues such as the neurosecretory cells of the adrenal medulla.

In considering how these kinetic effects arise, it is useful to examine the data in the context of a model for receptor activation. We are limited in what is known about neuronal nicotinic receptors, but we may begin by applying some of the information which is known about muscle AChRs. Numerous similarities exist between these neuronal receptors and what has been described for muscle receptors. For example, as with neuronal receptors, in all preparations of muscle AChR which have been studied (with adequate temporal resolution), two open states have been observed (for example: Sine & Steinbach, 1984, 1986*a*, *b*; Takeda & Trautmann, 1984; Colquhoun & Sakmann, 1985; Labarca *et al.* 1985; Papke & Oswald, 1989). One open state appears as brief isolated events, and the other is longer and often grouped in bursts. With muscle receptors, as with the $\alpha_3\beta_4$-receptors, the relative expression of these two open states is influenced by agonist concentration, which led to the suggestion that the brief openings may, at least in part, arise from singly liganded channels and that the longer-lived open state in muscle receptors is associated with doubly liganded receptors.

We cannot be sure of the number of agonist binding sites (i.e. α-subunits) which are present in neuronal receptors. Our previous work provides some evidence to support the idea that the different channel types we observed may in fact be associated with receptors of different subunit composition (Papke *et al.* 1989). The fact that at least two modes of activation exist for these receptors (i.e. two open states) and that the relative expression of these open states is influenced by agonist concentration suggests that a minimum of two α-subunits may be present in the neuronal receptors observed in these experiments.

As with muscle receptors, at concentrations of ACh $\geqslant 1\ \mu$M the total amount of current arising from the activation of the brief open state of the neuronal receptors is small compared to that associated with the long-lived open state ($\leqslant 6\%$),

consistent with the idea that the longer-lived open state is of greater functional significance. Therefore it is of interest to derive the rate constants for transitions associated with the long-lived open state in terms of a kinetic model of bursts. Crucial to such a model is the identification of that closed state which immediately precedes the first opening of a burst and which is entered upon the termination of a burst on the path to long-lived interburst closed states. Specifically, the question is whether such closed time is represented in our distributions by the closures fitted to $\tau_{c,1}$ or $\tau_{c,2}$. The analogous question is critical and remains controversial with regard to the activation of muscle AChR. Similar components exist in the closed time distributions of muscle receptors, and studies have concluded that for the mouse muscle receptor in BC3H-1 cells at room temperature (Papke & Oswald, 1987) or for receptors found at the frog neuromuscular junction (Colquhoun & Sakmann, 1985) the $\tau_{c,1}$ closures represent dwells in the doubly liganded closed state preceding the full open state. However, other studies of the mouse muscle receptor, in BC3H-1 cells at 11 °C (Sine & Steinbach, 1986*b*), or functionally expressed in *Xenopus* oocytes (Lo, Pinkham & Stevens, 1990) have suggested that the fastest class of closures represents excursions to a state outside the activation pathway (interruptions).

In the present study we observe that an increase in agonist concentration affects the number but not the duration of the $\tau_{c,2}$ closures. This would be consistent with a true intraburst closed state and inconsistent with a closed state with less than full agonist occupancy, since the dwell time in such a state would be decreased in the presence of higher agonist concentrations. Therefore we have chosen to use a model adapted from that which is applied to the behaviour of mouse muscle receptors expressed in oocytes by Lo *et al.* (1990). While this scheme is very simplified, omitting desensitized and other long-lived closed states, it is a useful model of the basic transitions within bursts of activity. The model assumes that the $\tau_{c,2}$ closures represent the closed state preceding opening (state 'C' below) and that $\tau_{c,1}$ closures represent a closed state outside the direct path of activation (state 'I' in the scheme below).

$$A + R \underset{}{\overset{k^-}{\rightleftharpoons}} C \underset{\beta}{\overset{\alpha}{\rightleftharpoons}} O \underset{I_f}{\overset{I_b}{\rightleftharpoons}} I.$$

In this scheme 'O' represents the long-lived open state and bursts occur as transitions between 'C', 'O', and 'I'. The rate of channel closing is α; I_f is the forward interruption rate. We have used this scheme to calculate the rate constants in Table 2. $\tau_{c,2}$ is equal to $1/(\beta + k^-)$ and the number of $\tau_{c,2}$ closures per burst equals β/k (see Methods). I_b, which is not included in the table, is equal to $1/\tau_{c,1}$ and is the same for both $\alpha_3\beta_4$- and $\alpha_3\beta_2$-receptor types.

If this simple model is adequate for describing the bursting behaviour of these receptors then the $\alpha_3\beta_4$-receptors differ from the $\alpha_3\beta_2$-subunit primary channel type in the kinetics of agonist dissociation and the channel opening rate. This would be consistent with a major influence on the behaviour of channels in the fully liganded closed state. Channels with the β_2-subunit would be more likely to dissociate from the agonist and fail to open, while β_4-channels would have a higher relative probability to open and also to re-open after closure. Additionally, the longer *apparent open times* of $\alpha_3\beta_4$-receptors may arise from both slower closing rates and fewer transitions to the interrupted state.

Recent studies (Blount & Merlie, 1989; Pedersen & Cohen, 1990) have provided evidence that the agonist binding sites on nicotinic receptors from the *Torpedo* electric organ may actually be at the interface of the α-subunits with the γ-and δ-subunits. An effect of the β_4-subunit on the kinetics of agonist binding to the α_3-subunit might occur as a steric interaction between a portion of the β_4-subunit and

TABLE 2. Rate constants

	Interruption rate	Closing rate (α)	Opening rate (β)	Agonist off-rate (k^-)
$\alpha_3\beta_4$-subunit primary type	247 ± 99	137 ± 66	304 ± 112	197 ± 47
$\alpha_3\beta_4$-subunit secondary type	277 ± 60	178 ± 79	353 ± 62	215 ± 56
$\alpha_3\beta_2$-subunit primary type	501 ± 100	261 ± 51	229 ± 73	367 ± 74

All values are means $\pm$ S.E.M.; units are s^{-1}.

the agonist binding site on the α_3-subunit. Alternatively the interactions between the α_3- and the β-subunits might be more complex, perhaps involving conformational influences of the β-subunit on the α_3-subunit or the entire ion channel protein.

The question arises whether the observation of different channel types from the pairwise expression of neuronal nicotinic subunits in oocytes means that this form of ectopic expression may give rise to abnormal forms of nicotinic receptors due to minimal constraints in the oocytes on the ways in which subunits assemble to form receptors. It is reasonable to imagine that *in vivo*, patterns of subunit assembly may be influenced by interaction with cytoskeletal structure, synaptic architecture, additional nicotinic subunits, or other cellular elements. However, numerous results from cells in tissue culture have also reported heterogeneous populations of neuronal nicotinic receptors. Up to three channel types have been reported in PC12 cells (Bormann & Matthaei, 1983) and as many as seven different types have been reported in chick sympathetic neurons (Moss, Schuetze & Role, 1989). This suggests that the multiple conductance types observed in the oocyte experiments reported here may be physiologically relevant.

The secondary channel type we observed for the $\alpha_3\beta_4$-receptor has the unusual feature that its activation properties change during the recording procedure, suggesting that it may be the target for either intracellular or surface modulations. This channel type seems to exhibit either two or three open states such that when the third open state is facilitated, even longer burst durations can result. The basis for such a change in channel behaviour is unclear, and the fact that the channel(s) used for the cluster analysis showed progressive rather than stepwise changes in behaviour is somewhat puzzling. One might expect that the results of a single modification such as an intracellular phosphorylation would be a rapid and stepwise change in channel properties. Our observations suggest that the change in channel properties may be associated with a slow exponential relaxation between a normal and a potentiated state. Alternatively, such a gradual change in receptor properties might reflect co-operative effects arising from multiple intracellular phosphorylations or the slow saturation of a number of low-affinity modulatory sites for the agonist. However, under conditions of stationary agonist concentration a process involving low-affinity sites for the agonist should reach an equilibrium and then result in essentially stable

behaviour. Whatever the mechanism, this non-stationary behaviour of the secondary channel type explains a large amount of the variability observed in the kinetic behaviour of the secondary type channels. For example, in Fig. 5, while the value for the average ratio of openings to bursts converges nicely with the primary and tertiary type channels, there is far more scatter in the data for the secondary type channels.

In conclusion we have shown that the subunit structure of ion channels is of critical importance to the behaviour of neurotransmitter receptors. Neuronal nicotinic receptors with relatively long open times and burst durations have been described in chromaffin cells (Fenwick, Marty & Neher, 1982; Clapham & Neher, 1984), and sympathetic neurons (Moss *et al.* 1989). These properties are correlated with the expression of the β_4-subunit in these tissues (I. Hermans-Borgmeyer, personal communication) as well as in other elements of the peripheral nervous system.

We would like to thank Dr Robert Duvoisin for making the β_4-subunit clone available to us prior to its publication. We also thank Drs Robert Duvoisin, Irm Hermans-Borgmeyer, Robert Oswald, John Bekkers, Richard Hume and Chuck Stevens for their useful comments and/or stimulating discussions. R.L.P. would also like to thank Dr Jim Boulter for his patient tutelage in the mysteries of Molecular Biology, past, present and future. Additionally we thank Dr Don Fredkin for writing the Excel Macro used for burst analysis. This work was in part supported by a J. Arron fellowship (to R.L.P.), a NIMH post-doctoral fellowship to R. L. P., a grant from the Muscular Dystrophy Association, and NIH grant number 5 R01 NS11549-17-21 to S.F.H. as well as funds provided by the Cigarette and Tobacco Surtax Fund of the State of California through the Tobacco-Related Research Program of the University of California.

REFERENCES

BLOUNT, P. & MERLIE, J. P. (1989). Molecular basis of two nonequivalent ligand binding sites of the muscle nicotinic acetylcholine receptor. *Neuron* **3**, 349–357.

BORMANN, H. & MATTHAEI, H. (1983). Three types of acetylcholine-induced single channel currents in clonal rat pheochromocytoma cells. *Neuroscience Letters* **40**, 193–197.

BOULTER, J., CONNOLLY, J., DENERIS, E., GOLDMAN, D., HEINEMANN, S. & PATRICK, J. (1987). Functional expression of two neuronal nicotinic acetylcholine receptors from cDNA clones identifies a gene family. *Proceedings of the National Academy of Sciences of the USA* **84**, 7763–7767.

BOULTER, J., EVANS, K., GOLDMAN, D., MARTIN, G., TRECO, D., HEINEMANN, S. & PATRICK, J. (1986). Isolation of a cDNA clone coding for a possible neural nicotinic acetylcholine receptor alpha subunit. *Nature* **319**, 368–374.

CLAPHAM, D. E. & NEHER, E. (1984). Substance P reduces acetylcholine-induced currents in isolated bovine chromaffin cells. *Journal of Physiology* **347**, 255–277.

COLQUHOUN, D. & SAKMANN, B. (1985). Fast events in single-channel currents activated by acetylcholine and its analogues at frog muscle end-plates. *Journal of Physiology* **369**, 501–557.

CONNOLLY, J. G. (1989). Mini review: Structure–function relationships in nicotinic acetylcholine receptors. *Comparative Biochemistry and Physiology* A **93**, 221–231.

COUTURIER, S., BERTRAND D., MATTER, J. M., HERNANDEZ, M. C., BERTRAND, S., MILLAR, N., VALERA, S., BARKAS, T. & BALLIVET, M. (1990*a*). The developmentally regulated chick neuronal nicotinic acetylcholine receptor subunit alpha7 assembles into a homo-oligomeric channel blocked by alpha-bungarotoxin. *Neuron* **15**(6), 847–856.

COUTURIER, S., ERKAMN, L., VALERA, S., RUNGGER, D., BERTRAND, S., BOULTER, J., BALLIVET, M. & BERTRAND, D. (1990*b*). Alpha5, alpha3, and non-alpha3: Three clustered avian genes encoding neuronal nicotinic acetylcholine receptor related subunits. *Journal of Biological Chemistry* **265**, 17560–17567.

DENERIS, E. S., CONNOLLY, J., BOULTER, J., PATRICK, J. & HEINEMANN, S. (1988). Primary structure and expression of β_2: A novel subunit of neuronal nicotinic acetylcholine receptors. *Neuron* **1**, 45–54.

DUVOISIN, R. M., DENERIS, E. S., PATRICK, J. & HEINEMANN, S. (1989). The functional diversity of the neuronal nicotinic acetylcholine receptors is increased by a novel subunit: β_4. *Neuron* **3**, 487–496.

FENWICK, E. M., MARTY, A. & NEHER, E. (1982). A patch-clamp study of bovine chromaffin cells and of their sensitivity to acetylcholine. *Journal of Physiology* **331**, 577–597.

GOLDMAN, D., DENERIS, E., KOCHHAR, A., BOULTER, J., PATRICK, J. & HEINEMANN, S. (1987). Members of a nicotinic acetylcholine receptor gene family are expressed in different regions of the mammalian central nervous system. *Cell* **48**, 965–973.

HAMILL, O. P., MARTY, A., NEHER, E., SAKMANN, B. & SIGWORTH, F. J. (1981). Improved patch-clamp techniques for high-resolution current recording from cells and cell-free membrane patches. *Pflügers Archiv* **391**, 85–100.

JARAMILLO, F. & SCHUETZE, S. M. (1988). Kinetic differences between embryonic- and adult-type acetylcholine receptors in rat myotubes. *Journal of Physiology* **396**, 267–296.

LABARCA, P., MONTAL, M. S., LINDSTROM, J. M. & MONTAL, M. (1985). The occurrence of long openings in the purified cholinergic receptor channel increases with acetylcholine concentration. *Journal of Neuroscience* **5**, 3409–3413.

LO, D. C., PINKHAM, J. L. & STEVENS, C. F. (1990). Role of a key cysteine in the gating of the acetylcholine receptors. *Neuron* **5**(6), 857–866.

LUETJE, C. W. & PATRICK, J. (1991). Both alpha and beta subunits contribute to the agonist sensitivity of neuronal nicotinic acetylcholine receptors. *Journal of Neuroscience* **11**(3) 837–845.

MOSS, B. L., SCHUETZE, S. & ROLE, L. W. (1989). Functional properties and developmental regulation of nicotinic acetylcholine receptors on embryonic chick sympathetic neurons. *Neuron* **3**, 597–607.

PAPKE, R. L., BOULTER, J., PATRICK, J. & HEINEMANN, S. (1989). Single channel currents of rat neuronal nicotinic acetylcholine receptors expressed in *Xenopus laevis* oocytes. *Neuron* **3**, 589–596.

PAPKE, R. L. & OSWALD, R. E. (1989). Mechanisms of noncompetitive inhibition of acetylcholine-induced single channel currents. *Journal of General Physiology* **93**, 785–811.

PEDERSEN, S. E. & COHN, J. B. (1990). *d*-Tubocurarine binding sites are located at the α-γ and α-δ subunit interfaces of the nicotinic acetylcholine receptor. *Proceedings of the National Academy of Sciences of the USA* **87**, 2785–2789.

SIGWORTH, F. J. & SINE, S. M. (1987). Data transformation for improved display and fitting of single channel dwell time histograms. *Biophysical Journal* **52**, 1047–1054.

SINE, S. M. & STEINBACH, J. H. (1984). Activation of a nicotinic acetylcholine receptor. *Biophysical Journal* **45**, 175–185.

SINE, S. M. & STEINBACH, J. H. (1986*a*). Acetylcholine receptor activation by a site-selective ligand. *Journal of Physiology* **370**, 357–379.

SINE, S. M. & STEINBACH, J. H. (1986*b*). Activation of acetylcholine receptors on clonal mammalian BC3H-1 cells by low concentrations of agonist. *Journal of Physiology* **373**, 129–162.

TAKEDA, K. & TRAUTMANN, A. (1984). A patch-clamp study of the partial agonist actions of tubocurarine on rat myotubes. *Journal of Physiology* **349**, 353–374.

WADA, E., WADA, K., BOULTER, J., DENERIS, E. S., HEINEMANN, S., PATRICK, J. & SWANSON, L. (1989). The distribution of alpha2, alpha3, alpha4, and beta2 neuronal nicotinic subunit RNAs in the central nervous system. A hybridization histochemical study in the rat. *Journal of Comparative Neurology* **284**, 314–335.

WADA, K., BALLIVET, M., BOULTER, J., CONNOLLY, J., WADA, E., DENERIS, E. S., BOULTER, J., SWANSON, L. W., HEINEMANN, S. & PATRICK, J. (1988). Functional expression of a new pharmacological subtype of brain nicotinic acetylcholine receptor. *Science* **240**, 330–334.